

**This is the accepted manuscript version of the contribution published as:**

**Liu, X., Wu, L., Kümmel, S., Merbach, I., Lal, R., Richnow, H.H.** (2020):  
Compound-specific isotope analysis and enantiomer fractionation to characterize the  
transformation of hexachlorocyclohexane isomers in a soil–wheat pot system  
*Environ. Sci. Technol.* **54** (14), 8690 – 8698

**The publisher's version is available at:**

<http://dx.doi.org/10.1021/acs.est.9b07609>



14 **Abstract**

15 The uptake by plant from soil is one of the first steps for hexachlorocyclohexane isomers (HCHs)  
16 to enter the food web. However, the HCH transformation associated with the uptake process is still  
17 not well understood. Therefore, a soil-wheat pot experiment was conducted to characterize the  
18 HCH transformation during wheat growth using compound-specific isotope analysis (CSIA) and  
19 enantiomer fractionation. The results showed that the  $\delta^{13}\text{C}$  and  $\delta^{37}\text{Cl}$  values of  $\beta$ -HCH remained  
20 stable in soil and wheat, revealing no transformation. In contrast, an increase of  $\delta^{13}\text{C}$  and  $\delta^{37}\text{Cl}$   
21 values of  $\alpha$ -HCH indicated its transformation in soil and wheat. A shift of the enantiomer fraction  
22 (EF) (-) from 0.50 to 0.35 in soil at jointing stage and 0.35 to 0.57 at harvest stage suggested that  
23 the preferential transformation of enantiomers varied at different growth stages. Based on the dual  
24 element isotope analysis, the transformation mechanism in soil-wheat system was different from  
25 that in wheat in hydroponic systems. The high abundance of HCH degraders, *Sphingomonas* sp. and  
26 *Novosphingobium* sp., was detected in the  $\alpha$ -HCH treated rhizosphere soil, supporting the potential  
27 for biotransformation. The application of CSIA and EF allows characterizing the transformation  
28 of organic pollutants such as HCHs in the complex soil-plant systems.

## 29 INTRODUCTION

30 A large amount of hexachlorocyclohexane (HCH) muck (mostly containing  $\alpha$ - and  $\beta$ -HCH) was  
31 dumped in the environment during the production of Lindane ( $\gamma$ -HCH) <sup>1</sup>. Although Lindane was  
32 banned according to the Stockholm convention in 2009 <sup>2</sup>, the HCH contamination has spread  
33 globally, and the bioaccumulation and bio-magnification of HCHs were found in the food web.  
34 There are high concerns about the accumulation of HCHs in food web as human could be the final  
35 receptors. HCHs have been detected in human milk <sup>3</sup>, blood <sup>4</sup>, and fatty tissues <sup>5,6</sup>. Plant uptake  
36 from soil is one of the first steps for HCHs to enter the food web, leading to increasing human  
37 exposure risks. The uptake of HCHs by roots potentially with the transpiration stream, or by leaves  
38 from the gas phase has been discussed before <sup>7,8</sup>. Bioconcentration, which is defined as the ratio  
39 between the concentration of HCHs in wheat tissues and that of in the host soil, was overestimated  
40 when comparing model data with the data from a field experiment <sup>8</sup>. This could be due to the  
41 underestimation of the HCH transformation in plants in these models. Therefore, the models need  
42 to be improved by taking the transformation into account. However, the transformation of HCHs  
43 associated with their uptake process in the soil-plant system is still not well understood. The key  
44 question is which factors control the uptake of HCH into plants, and how the uptake is  
45 accompanied by the biotransformation either by microorganisms in the soil, endophytes within  
46 plants, or metabolic processes in plants.

47 The transformation of HCHs by soil microorganism was reported in the literature <sup>9,10</sup>. There are  
48 no reports about the endophytes and enzymes involved in the transformation of HCHs in plant,  
49 however, the transformation of other organic contaminants during uptake into plants has been  
50 controversially discussed. For instance, polycyclic aromatic hydrocarbons could be degraded in

51 biofilms on root surfaces and by endophytes as demonstrated for phenanthrene<sup>11-13</sup>. Ibuprofen  
52 could be transformed by plant-derived enzymes<sup>14</sup>.

53 Compound-specific isotope analysis (CSIA) has been considered to be a promising tool for  
54 characterizing the fate of HCHs in the field<sup>15,16</sup>. Several carbon isotope enrichment factors  
55 obtained from the pure culture of *Sphingomonas* sp. could be applied to characterize the aerobic  
56  $\alpha$ -HCH degradation<sup>17,18</sup>. Enantiomer fraction (EF) is an indicator of the biotransformation of chiral  
57 compounds and can indicate the selective uptake processes of specific enantiomers<sup>19</sup>. Several  
58 studies have combined the CSIA and EF to characterize the microbial transformation of  $\alpha$ -HCH at  
59 the laboratory scale and in aquifers at landscape level<sup>17,20</sup>. The application of CSIA and EF  
60 methods in soil-plant system could give impetus for characterizing the fate of organic pollutants  
61 in complex systems, and it is a huge step towards the development of the methods.

62 Wu et al.<sup>21</sup> analyzed the isotope composition of HCHs in plants and soil to monitor the  
63 transformation of HCHs in a contaminated field. However, it is difficult to detect the degradation  
64 of HCHs in soil and in plants because many variable growth conditions in the field, such as dry/wet  
65 seasons and nutrition for plant growth, can influence the uptake processes. A hydroponic  
66 experiment conducted under sterile conditions with wheat provided the evidence of  $\alpha$ -HCH  
67 transformation in plant during uptake along with the water flow from root to leaves<sup>22</sup>. However,  
68 the transformation of HCHs during uptake from soil to plant could be also affected by the  
69 rhizosphere microbiome.

70 Therefore, a soil pot experiment was conducted to systematically investigate the isomer- and  
71 enantiomer-specific uptake, possible turnover of HCHs in soil and in wheat using CSIA and EF.  
72 We selected three wheat growth stages covering the whole period of wheat growth to investigate

73 the influence of plant growth on the transformation of HCHs in the soil-plant system. The HCH  
74 transformation was examined by the HCH concentration, isotope fractionation as well as  
75 enantiomer fractionation in soil and wheat tissues. In addition, the microbial community in the  
76 bulk and rhizosphere soil at the harvest stage was evaluated to elucidate the transformation of  
77 HCHs in soil. The understanding of the HCH transformation in soil-plant systems could provide  
78 valuable details for the development of phytoremediation strategies.

## 79 **MATERIALS AND METHODS**

80 The sources and quality of chemicals are provided in the S1 (SI).

81 **Seeds and Plant Exposure to HCHs in the Soil.** Wheat (cultivar *Quintus* of *Triticum aestivum* L.)  
82 was used as the test plant and the seeds were obtained from the breeder Saaten-Union GmbH  
83 (Isernhagen, Germany). The soil was provided by LAV Technische Dienste GmbH (Markranstädt,  
84 Germany). The major physicochemical properties of the sandy soil are: total organic carbon 2.2%,  
85 pH 7.9, soil texture is sandy silt soil with 11 % clay, 49 % silt, 40 % sand. The soil is classified as  
86 Luvisol (World Reference Base). The parent material is loess formed in a temperate zone located  
87 in the Saxony (Germany).

88 The experiment was conducted in the glass house of the research station of the UFZ in Bad  
89 Lauchstädt. The sandy soil was air-dried and sieved through a 5 mm mesh before usage. Then, 250  
90 g of soil was spiked with 210 mg of  $\alpha$ - and  $\beta$ -HCH solutions in acetone individually. When the  
91 acetone was evaporated, the spiked soil was mixed with non-spiked soil with the addition of basic  
92 fertilization (6g  $\text{CaHPO}_4 \cdot 2\text{H}_2\text{O}$  as solid; 4.46g  $\text{K}_2\text{SO}_4$ , 5.125g  $\text{MgSO}_4 \cdot 7\text{H}_2\text{O}$ , 5.72g  $\text{NH}_4\text{NO}_3$ , and  
93 0.15g  $\text{FeCl}_3$  as solution; 3ml Hoagland micro nutrition solution). Afterwards, the soil was  
94 homogenized thoroughly before packed into pots (7kg soil per pot) and then equilibrated at room

95 temperature for several days at 60% of the water holding capacity. The final concentration of HCH  
96 isomers was theoretically 30 mg kg<sup>-1</sup>. In each pot, 12 seeds were grown uniformly and at last 9  
97 seedlings were left after germination. During the whole period of wheat growth, the water content  
98 of soil was maintained as 60% of the maximum water content of soil. The treatments for the  
99 individual experiment were as follows: 30 mg kg<sup>-1</sup> α-HCH spiked sandy soil with wheat (α-HCH  
100 spiked treatment), 30 mg kg<sup>-1</sup> β-HCH spiked sandy soil with wheat (β-HCH spiked treatment);  
101 non-spiked sandy soil with wheat (Control). Each treatment had 4 replicates. The pots of different  
102 treatments were placed randomly. The soil surface in each pot was covered by a thin layer of 2-  
103 cm silica sand (150-380 um) to prevent the transportation of soil particles directly to the leave  
104 surface by air and to reduce the HCH exchange between soil-air interface as reported for  
105 hexabromocyclododecane isomers (HBCDs) <sup>23</sup>.

106 **Sampling of HCHs from the Soil and Plant.** Wheat grew for 102 days from April to July in 2018.  
107 At the jointing (48 days), heading (64 days) and harvest stage (102 days), soil and plant were  
108 sampled. The soil samples were separated into bulk soil and rhizosphere soil. The whole soil and  
109 root system was gently crushed and loosely held soil was separated by shaking. This is referred as  
110 bulk soil. The remaining tightly held soil particles were considered as the rhizosphere soil, and  
111 were removed by shaking in a plastic bag <sup>24</sup>. A small portion of the soil samples were frozen at -  
112 20 °C for metagenomics analysis. The remaining soil samples were lyophilized for further  
113 treatment. An aliquot of the initial soil before planting were taken and named as the original soil  
114 for comparison. After taking the rhizosphere soil, plant samples were washed thoroughly for 4  
115 times using sterilized water and then separated into root, stem, leaf, spike and grain. Plant samples  
116 were lyophilized and ground for further treatment.

117 **Extraction and Clean-up of HCHs from Soil and Plant Samples.**

118 The method for the extraction and clean-up of HCHs in soil and plant has been developed  
119 previously for isotope analysis <sup>25</sup>. The details are shown in S2 (SI).

120 **DNA extraction and sequencing.** The genetic analysis was carried out by isolating the  
121 metagenomic DNA directly from the soil which contains representation from both active and  
122 inactive bacteria residing in the respective soil samples. DNA was extracted from soil using  
123 DNeasy PowerSoil Kit – QIAGEN (Cat no. 12888-50) as described in the manufacturer’s  
124 instructions. The quality of DNA was assessed using a NanoDrop ND-1000 (Thermo Scientific).  
125 The shotgun sequencing was done in collaboration with Phixgen Pvt. Ltd. using an Illumina HiSeq-  
126 2500 platform with paired-end 150bp read length.

127 **Analytical Methods.** *Concentration Analysis.* An Agilent 6890 series GC (Agilent Technologies,  
128 USA) equipped with a flame ionization detector (FID) was used to determine the concentration of  
129 HCHs throughout the study. The details are shown in S3 (SI).

130 *Isotope Analysis.* The isotope composition of element (E) was reported as  $\delta$  notation in parts per  
131 thousand (‰) relative to the international standard scale according to eq 1.

132 
$$\delta E_{sample} = \frac{R_{sample}}{R_{standard}} - 1 \quad (1)$$

133  $R_{sample}$  and  $R_{standard}$  are the  $^{13}\text{C}/^{12}\text{C}$  and  $^{37}\text{Cl}/^{35}\text{Cl}$  ratios of the sample and the standard, respectively.

134 Carbon isotope composition ( $\delta^{13}\text{C}$ ) was analyzed by a gas chromatograph-combustion-isotope  
135 ratio mass spectrometer (GC-C-IRMS), where a GC (7890A, Agilent Technologies, USA) was  
136 connected through a GC-IsoLink and a ConFlo IV interface (Thermo Fisher Scientific, Germany)  
137 to a MAT 253 IRMS system (Thermo Fisher Scientific, Germany). The details are shown in S3  
138 (SI).



139 Chlorine isotope composition ( $\delta^{37}\text{Cl}$ ) was analyzed using a gas chromatograph coupled with a  
140 multiple-collector inductively coupled plasma mass spectrometer (GC-MC-ICPMS), as recently  
141 described elsewhere <sup>26</sup>. The details are shown in S3 (SI).

142 *Enantiomer Analysis.* The Enantiomer fraction (EF) (-) is defined as  $A^- / (A^+ + A^-)$ , where  $A^+$  and  
143  $A^-$  correspond to the peak area or concentrations of (+) and (-) enantiomers. The EF of  $\alpha$ -HCH  
144 was analyzed by gas chromatograph mass spectrometer (GC-MS) (Agilent Technologies 7890A  
145 for GC and 5975C for MS, USA) equipped with a  $\gamma$ -DEX 120 chiral column (30 m  $\times$  0.25 mm  $\times$   
146 0.25  $\mu\text{m}$ , Supelco, Bellefonte, PA, USA) <sup>27</sup>. The details are shown in S3 (SI).

147 *Metabolites Analysis.* The metabolites (1,3,4,5,6-pentachlorocyclohexene and 1,2,4-  
148 trichlorobenzene) of HCHs in plant and soil were measured by a GC-MS as mentioned above. The  
149 details are shown in S3 (SI).

150 *Bioconcentration Factors.* Bioconcentration factors (BCFs) for root (RCF), stem (SCF), leaf  
151 (LCF), spike (SPCF) and grain (GCF) were calculated as the ratio between the concentration of  
152 HCHs in wheat tissues and that of in the host soil to study the translocation of HCH in plants. The  
153 HCH concentration normalized to dry weight was used for calculation.

154 *Metagenomics Analysis.* The reads obtained after whole metagenome sequencing using Illumina  
155 platform were trimmed and analyzed. The details of method are reported in S3 (SI).

156 *lin gene profiling and their relative abundance.* The sequences for the *lin* genes from the complete  
157 genomes of *Sphingobium japonicum* UT26 and *Sphingobium indicum* B90A were taken as  
158 reference for assessing the presence of *lin* genes required for the transformation of HCHs. The  
159 details of method are reported in S3 (SI).

160 *Dual elements isotope analysis.* The Lambda ( $\Lambda$ ) value was used to distinguish different  
161 transformation mechanisms in a complex system.  $\Lambda$  is defined as the slope of the regression line  
162 of the isotope fractionation of two elements during a transformation process <sup>28</sup>.

163 *Statistical analysis.* The HCH concentration data in soil at different stages was analyzed  
164 statistically using analyses of variance (ANOVA) and Least Significance Difference post-hoc  
165 comparison testing with the SPSS soft- ware v19.0. The HCH concentration data in soil at the  
166 same stage and EF(-) data were analyzed using independent *t*-test ( $p<0.05$ ) with the SPSS soft-  
167 ware v19.0.

## 168 **Results and Discussion**

169 **Concentration of HCHs in the Soil-plant System.** The yield wheat biomass was not influenced  
170 by the HCH spiking and details were shown in S4 and Table S1 (SI). The concentration of  $\alpha$ -HCH  
171 in the bulk soil decreased from an initial concentration of  $21.4 \pm 0.6 \text{ mg kg}^{-1}$  to  $18.4 \pm 1.5 \text{ mg kg}^{-1}$   
172 <sup>1</sup> at the jointing stage, to  $13.8 \pm 0.3 \text{ mg kg}^{-1}$  at the heading stage, and to  $11.9 \pm 0.3 \text{ mg kg}^{-1}$  at the  
173 harvest stage (Fig. S1a.). The loss of HCHs in the bulk soil was a result of the evaporation, uptake,  
174 biotransformation, and evapotranspiration by plant. There was no difference of the  $\alpha$ -HCH  
175 concentration in the rhizosphere soil at different stages but it was significantly lower than that in  
176 the bulk soil at the same stage (Fig. S1a.), which is coherent with the former report <sup>24</sup>. This was a  
177 result of higher abundance of HCH-degrading microorganisms, such as species of the genera  
178 *Sphingomonas* and *Novosphingobium* in the rhizosphere (the data was shown in below). Exudates  
179 from roots in the rhizosphere could support the number and diversity of microorganisms, leading  
180 to a larger potential for transforming organic pollutants <sup>29</sup>.

181 Compared with the initial concentration ( $24.6 \pm 0.8 \text{ mg kg}^{-1}$ ), the concentration of  $\beta$ -HCH in the  
182 bulk soil decreased to  $23.9 \pm 0.6 \text{ mg kg}^{-1}$  at the jointing stage, and significantly decreased to  $22.5$   
183  $\pm 0.7 \text{ mg kg}^{-1}$  at the heading stage and  $21.8 \pm 0.5 \text{ mg kg}^{-1}$  at the harvest stage, which was much  
184 higher than that for  $\alpha$ -HCH (Fig. S1b.). Additionally, the concentration of  $\beta$ -HCH in the  
185 rhizosphere soil was nearly identical with that in the bulk soil in the same experimental phase,  
186 indicating that  $\beta$ -HCH may not be transformed preferentially in rhizosphere (Fig. S1b.).

187 No HCHs could be detected in the non-spiked control pots, suggesting the uptake of HCHs by leaf  
188 from the air in the present experiment could be neglected. In the spiked treatments, HCHs could  
189 be observed in all wheat tissues at three growth stages with the highest concentration in the roots  
190 followed by the stems and the lowest in the leaves. This indicates that HCHs were translocated to  
191 all parts of the wheat after uptake by roots (Fig. S1c and S1d.). The concentration of  $\beta$ -HCH in  
192 spike and grain was smaller than  $\alpha$ -HCH, suggesting  $\alpha$ -HCH was translocated to a larger extent to  
193 the upper part of wheat than  $\beta$ -HCH at the stage of harvest.

194 The BCFs of  $\alpha$ -HCH was higher than that of  $\beta$ -HCH, which could be related to the different  $K_{ow}$   
195 of HCHs (Table S2, SI.). The  $\alpha$ -HCH has a lower  $K_{ow}$  (lower hydrophobicity) than  $\beta$ -HCH<sup>30</sup> and  
196 therefore may be easier to translocate along with the water flow in plant. The RCF and SCF of  
197 both  $\alpha$ -HCH and  $\beta$ -HCH were increased along with the wheat growth and the highest value was  
198 observed at the harvest stage (Table S2, SI.). In contrast, the LCF values were the highest at the  
199 heading stage (Table S2, SI.). This suggested that several processes were involved in the  
200 accumulation of HCHs in leaves. Previous studies showed that the accumulation of HCHs in plant  
201 leaves was a result of the combination of uptake by root and foliar uptake from the air<sup>7,8</sup>. In this  
202 study, the only relevant uptake of HCHs was via the roots. However, chemicals in plant leaves  
203 might be exchanged to the air with the evapotranspiration in contrast to uptake by air<sup>31</sup>.

204 Furthermore, during the overall translocation progress in the plant, HCHs will be internally  
205 translocated between different plant organs particularly during grain filling. At the harvest stage,  
206 the HCHs may be translocated along with biological material to the grain as the physiology of the  
207 plant is targeting on grain filling, which may cause the decrease of the LCF and SPCF at the harvest  
208 stage.

209 **Carbon and Chlorine Isotope Fractionation of HCHs in the Soil-plant System.** The isotopic  
210 changes discussed in present study are attributed to the kinetic isotope fractionation, which results  
211 in a preferential degradation of the isotopically light molecules. There was no difference in  $\delta^{13}\text{C}$   
212 and  $\delta^{37}\text{Cl}$  values of  $\beta$ -HCH observed in the soil and wheat tissues compared to the  $\beta$ -HCH spiked  
213 to soil (Fig. 1a-d), revealing that  $\beta$ -HCH was not transformed in soil and wheat in this study.  
214 However, in the previous field study, a slight increase of  $\delta^{13}\text{C}$  value of  $\beta$ -HCH was observed in  
215 the bulk soil <sup>21</sup>. The reason for the difference could be that the  $\beta$ -HCH degrading microbial  
216 community in soil has been well developed in the field due to long time exposure to  $\beta$ -HCH. Thus,  
217  $\beta$ -HCH could be transformed prior to uptake into plant, leading to isotope enrichment of  $\beta$ -HCH  
218 residues in soil and some plants <sup>21</sup>. However, in this study, the experiment was conducted in 3  
219 months and the soil microbial community had not developed the ability for transforming  $\beta$ -HCH  
220 or enough abundance of  $\beta$ -HCH degrading bacteria in this relatively short period. The  $\delta^{13}\text{C}$  and  
221  $\delta^{37}\text{Cl}$  values of  $\beta$ -HCH showed that the translocation and accumulation of  $\beta$ -HCH by wheat did  
222 not change the C- and Cl-isotopic composition of  $\beta$ -HCH, thus the uptake alone could not affect  
223 the isotope composition as also was observed in the hydroponic experiments elsewhere <sup>22</sup>.

224 Since  $\alpha$ -HCH has similar physicochemical properties as  $\beta$ -HCH, the translocation only is unlikely  
225 to affect the isotope values of  $\alpha$ -HCH. Interestingly, an increase in  $\delta^{13}\text{C}$  value of  $\alpha$ -HCH was  
226 observed in both bulk and rhizosphere soil at different growth stages compared to the initial value

227 of -28.5 ‰ (Fig. 2a), especially at the harvest stage ( $\delta^{13}\text{C}$  value in the bulk and rhizosphere soil  
228 was -24.9 ‰ and -25.2 ‰, respectively). This indicates that  $\alpha$ -HCH was transformed both in the  
229 bulk and rhizosphere soil. An increase of  $\delta^{13}\text{C}$  value of  $\alpha$ -HCH was found from the jointing stage  
230 to the harvest stage in both bulk and rhizosphere soil (Fig. 2a), which could be related to the  
231 development of  $\alpha$ -HCH degrading bacteria along with the wheat growth. The result was consistent  
232 with a previous field study where the enrichment of  $^{13}\text{C}$  isotopes of  $\alpha$ -HCH in bulk soil were  
233 observed during plant growth compared to the HCH muck <sup>21</sup>.

234 Compared to the  $\delta^{13}\text{C}$  value of  $\alpha$ -HCH in soil, the  $\delta^{13}\text{C}$  value in wheat tissues at the jointing stage  
235 significantly increased up to 3 ‰ (Fig.2c.), especially in stem and leaf, implying that  $\alpha$ -HCH could  
236 be further transformed within wheat after uptake. The results are consistent with the observation  
237 of the  $\delta^{13}\text{C}$  increase of  $\alpha$ -HCH in wheat tissues in the early stage in a hydroponic system <sup>22</sup>. At the  
238 heading stage, an enrichment of  $^{13}\text{C}$  isotopes of  $\alpha$ -HCH in wheat tissues except stem was obtained  
239 compared to the soil. The transformation of  $\alpha$ -HCH in this study could be associated with the  
240 endophytes and plant-derived enzymes. The major roles of endophytes in the degradation of  
241 organic contaminants in *planta* are related to various factors such as chelating agents, siderophores,  
242 biosurfactants, low molecular weight organic acids, and various detoxifying enzymes <sup>32</sup>. Plant  
243 derived enzymes such as P450 monooxygenases, dehalogenase, glutathione S-transferases (GST),  
244 and glucosyltransferases (UGT) could play a role in the detoxification of organic pollutants <sup>33</sup>. For  
245 examples, hybrid poplar (*Populus spp.*), algae (*various spp.*), and parrot feather (*Myriophyllum*  
246 *aquaticum*) have been reported to produce dehalogenases for transforming DDT <sup>34</sup>.  
247 Polychlorinated biphenyls (PCBs) could be dehalogenated by sterile plant tissues <sup>35</sup>. The  
248 detoxification process of  $\gamma$ -HCH by *Phragmites australis* plants could be potentially be attributed  
249 to UGT enzymes in root and rhizome as well as by GST enzymes in leaf <sup>36</sup>. Endophytes which

250 have the possibility to promote the clean-up of HCHs were isolated from *Cytisus striatus* growing  
251 on HCH-contaminated soil<sup>37</sup>. Metabolite analysis revealed 1,3,4,5,6-pentachlorocyclohexene  
252 (PCCH) as a major metabolite of  $\alpha$ -HCH in both soil and plant (Fig. S2a), indicating a  
253 dehydrochlorination reaction of  $\alpha$ -HCH in soil and plant. 1,2,4- trichlorobenzene (1,2,4-TCB) was  
254 only found in plant tissues (Fig. S2b), suggesting further transformation by dehydrochlorination  
255 reaction in plant tissues. Other metabolites could not be detected by GC-MS which might be due  
256 to the low concentration. The metabolites are similar to those formed during HCH degradation by  
257 *Sphingomods* which are typical HCH degrading soil bacteria<sup>10</sup>, leading to the hypothesis that  
258 dehydrochlorination reaction of HCH in plants could be associated with the endophytic  
259 microorganisms in addition to plant-derived dehalogenase catalyzed reactions.

260 However, at the harvest stage, only  $\alpha$ -HCH in root showed an increased  $\delta^{13}\text{C}$  value and no  $\delta^{13}\text{C}$   
261 increase was observed in other wheat tissues compared to the soil. This indicated that the changes  
262 of the isotopic composition in the same tissues at different stages were mostly related to the plant  
263 activity. Firstly, it might be affected by the changes in enzyme activity and the community of  
264 endophytes due to the different plant growth conditions at different growth stages. Secondly, the  
265 HCH uptake from soil was a continuous process along with the water flow. At the early stage, the  
266 HCH concentration in wheat was low, therefore HCH showed a strong isotope fractionation  
267 indicating intensive transformation in plant. A larger amount of water was required at the later  
268 stages and therefore higher accumulation of HCH with low isotope fractionation indicated an  
269 overall lower transformation. The higher uptake of water led to larger translocation of HCH along  
270 with the water flow in plant, resulting in relatively lower transformation. However, the  
271 translocation of HCH along with the water flow should not affect the isotope fractionation as no  
272 bond change occurs in contrast to transformation. A potential isotope fractionation due to the

273 sorption of HCH on the plant cell wall or cell tissue is unlikely as the isotope fractionation caused  
274 by phase partitioning is low compared to the transformation<sup>38</sup>, therefore the isotope fractionation  
275 of HCH due to the transport in the plant could be neglected.

276 A consistent increase of  $\delta^{13}\text{C}$  value of  $\alpha$ -HCH was found in root along with the wheat growth (Fig.  
277 2c), indicating the larger transformation in root at the later stage. This was different from in other  
278 tissues which fluctuated along with the wheat growth. The isotope fractionation of HCH in root  
279 may be highly influenced by rhizosphere microorganisms which may have the potential to enter  
280 and colonize plant roots and contribute to the transformation in root<sup>39</sup>.

281 The development of  $\delta^{37}\text{Cl}$  pattern of  $\alpha$ -HCH in soil samples was similar with  $\delta^{13}\text{C}$ . An increasing  
282 enrichment of  $^{37}\text{Cl}$  isotopes of  $\alpha$ -HCH in the bulk and rhizosphere soil was observed along with  
283 the wheat growth (Fig. 2b.). The observation of the simultaneous enrichment in  $\delta^{13}\text{C}$  and  $\delta^{37}\text{Cl}$   
284 values revealed that a C-Cl bond was already cleaved during of  $\alpha$ -HCH transformation in soil to  
285 some extent. The  $\delta^{37}\text{Cl}$  pattern of  $\alpha$ -HCH in plant samples was also similar with  $\delta^{13}\text{C}$  (Fig. 2d.),  
286 indicating further C-Cl bond cleavage caused by plant endophytes or enzymes. Only the  $\delta^{37}\text{Cl}$  in  
287 grain was higher than its host soil, suggesting the transformation pathway of  $\alpha$ -HCH in grain was  
288 different from other wheat tissues.

289 **Enantiomer Fractionation of  $\alpha$ -HCH in the Soil-plant System.** Enantiomer fractionation could  
290 occur due to the biotransformation of chiral compounds<sup>40</sup>. Enantiomer fraction (EF) was applied  
291 as an indicator for characterizing the enantiomer fractionation process. In the present study, a  
292 significant change of EF in soil samples was noted at different wheat growth stages (Fig. 3.). At  
293 the jointing stage, EF (-) in the bulk and rhizosphere soil significantly decreased to  $0.349 \pm 0.002$   
294 and  $0.396 \pm 0.004$  respectively compared to the initial EF(-) of  $0.502 \pm 0.002$ . However, the EF (-)

295 in the bulk and rhizosphere soil significantly increased to  $0.544 \pm 0.001$  and  $0.556 \pm 0.004$  at the  
296 heading stage, and to  $0.559 \pm 0.010$  and  $0.566 \pm 0.003$  at the harvest stage. The results suggested  
297 a preferential biotransformation of (-)  $\alpha$ -HCH at the early stage and a preferential  
298 biotransformation of (+)  $\alpha$ -HCH at the later stages in soil.

299 *Spingobium indicum* B90A is a HCH degrader in soil and could show different preferential  
300 enantiomer transformation of  $\alpha$ -HCH in different conditions <sup>41,42</sup>. A recent study of the Lin  
301 enzymes revealed the preferential transformation of (-)  $\alpha$ -HCH in resting cells and crude extracts  
302 from the same strain and a pronounce isotope fractionation of LinA enzymes <sup>43</sup>. The large  
303 variability of enantiomer fractionation in bacteria, even the same bacteria, indicates that different  
304 growth phases (lag phase, log phase, and stationary phase) or different cultivation conditions can  
305 lead to changes in the activity of the Lin enzymes <sup>43</sup>. Therefore, reasons for the variation of EF in  
306 soil in present study could be due to that the different plant growth stages and release of root  
307 exudates influence the growth conditions of HCH-degrading microorganisms in soil and also  
308 change compositions of soil microbial community <sup>44</sup>, which may influence the preference  
309 transformation of enantiomers.

310 Unlike the shift of EF in soil at different stages, the EF in plant samples was more stable. At the  
311 jointing stage, the EF (-) in all wheat tissues was below 0.5 and higher than that in soil samples.  
312 At the heading stage, the EF (-) in root, stem and spike significantly increased to  $0.523 \pm 0.001$ ,  
313  $0.514 \pm 0.001$  and  $0.511 \pm 0.001$ , respectively, in contrast to that in leaf ( $0.482 \pm 0.002$ ). At the  
314 harvest stage, the EF (-) in root significantly increased to  $0.529 \pm 0.001$  and the EF (-) in stem  
315 ( $0.499 \pm 0.001$ ) was identical with racemic mixture. The EF (-) in other wheat tissues (leaf,  $0.477$   
316  $\pm 0.002$ ; spike,  $0.482 \pm 0.007$ ; grain,  $0.474 \pm 0.007$ ) was significantly lower than the racemic  
317 mixture. At the heading and harvest stages, all the EF (-) values in wheat tissues were lower than



318 that of in soil samples in the same stage. The variability of EF (-) in all wheat tissues at different  
319 stages varied from 0.449 to 0.529, which was smaller than that in soil. Except the root, all other  
320 tissues showed a preferential biotransformation of (-)  $\alpha$ -HCH at the harvest stage where its host  
321 soil showed a high preferential biotransformation of (+)  $\alpha$ -HCH. Similar observation was made in  
322 a recent field study<sup>21</sup>. The result indicated that the specific transformation of enantiomers in plant  
323 was different from soil. Possibly endophytes and enzymes in plant may also show different  
324 transformation pathway of enantiomers. The results may also suggest that the above-ground plant  
325 parts showing the enantiomer fractionation can be related to a mixture of processes e.g. plant-  
326 internal enantiomer specific transformation, continued uptake from soil, and plant-internal  
327 translocation during the growth. EF (-) in root increased from  $0.492 \pm 0.001$  to  $0.530 \pm 0.001$  along  
328 the wheat growth, which differed from the other wheats tissues but the trend was similar as in the  
329 soil. The reason may be that root took up  $\alpha$ -HCH with an enantiomer composition already affected  
330 by microorganism in the rhizosphere.

331 However, based on the obtained data in this study, it is difficult to further evaluate the specific  
332 transformation of enantiomers in plant, therefore the contribution of bacteria and plant cannot be  
333 distinguished. Further studies focusing on *in vivo* transformation experiment with plant-derived  
334 enzymes or endophytes would be needed to elucidate this aspect.

### 335 **Combined $\delta^{13}\text{C}$ and $\delta^{37}\text{Cl}$ Analysis for Characterizing HCHs in the Soil-plant System.**

336 Different reaction mechanisms involve chemical bonds containing different elements. Reaction  
337 mechanisms can therefore be differentiated using dual isotope plots that have different slopes  
338 indicating different reaction mechanisms in complex system<sup>28</sup>. The changes of  $\delta^{37}\text{Cl}$  Vs  $\delta^{13}\text{C}$   
339 values in soil and plant samples (except grain) could be described linearly with a linear regression  
340 slope ( $\Lambda$ ) of  $3.30 \pm 0.16$ , suggesting that the overall transformation processes of  $\alpha$ -HCH in the

341 soil-wheat system contributed to the similar mode of C-Cl bond cleavage (Fig. 4). The grain  
342 sample has a different isotope fractionation pattern, suggesting the mode of C-Cl bond cleavage in  
343 the grain was different from other wheat tissues. Based on the previous study<sup>22</sup>, a slope of  $1.75 \pm$   
344  $0.13$  was observed in the plant samples from a hydroponic system where plant metabolism is  
345 dominating the transformation pathway. The observation suggested that plant growing in soil pot  
346 experiment had different mode of C-Cl bond cleavage of  $\alpha$ -HCH compared to that in hydroponic  
347 experiment.

348 The fundamental difference between hydroponic and soil pot experiment is that the microbial  
349 activity in the rhizosphere obviously effects the correlation of  $^{13}\text{C}$  and  $^{37}\text{Cl}$  isotope fractionation  
350 implying contribution of different pathways.

### 351 **Microbial Community and Dynamics deciphered using Metagenomics Analysis**

352 Five soil samples including the original soil sample (OS), the bulk and rhizosphere soil of  $\alpha$ -HCH  
353 treatment at the harvest stage (BHA1 and RHA1), the bulk and rhizosphere soil of control at the  
354 harvest stage (BHC and RHC) were collected for the analysis of metagenomics. The  $\alpha$ -diversity  
355 analysis based on Shannon (H) and Simpson (D) index indicated that the original soil was the most  
356 abundant in species diversity followed by the rhizosphere soils *i.e.*, RHA and RHC (Fig. S3 and  
357 S4.). The bulk control soil represented the least species diversity, even less than the bulk soil  
358 treated with  $\alpha$ -HCH. This can be explained by the basis of selection pressure and one of such  
359 factors can be HCH. In the original soil without HCH pressure, all communities with or without  
360 tolerance to HCH can occupy the niches and hence the sample has a much larger diversity.

361 In addition, the  $\beta$ -diversity based on Bray-Curtis dissimilarity matrix also revealed that the original  
362 soil had the most diverse composition of bacteria, which significantly changed during the wheat

363 growth (Fig. S5.). The rhizosphere soil treated with  $\alpha$ -HCH had distinct bacterial community  
364 compared with the bulk soil and control rhizosphere soil (Fig. S5). The six most abundant genera  
365 across the five samples deciphered and the rhizosphere soil treated with  $\alpha$ -HCH (RHA1) clearly  
366 showed significant enrichment of two bacterial genera *viz.*, *Sphingomonas* and *Novosphingobium*,  
367 which were reported to either tolerate or degrade HCH <sup>45</sup> (Fig. S6 and S7) (PMID: 28567447,  
368 27581378). The genomic bins reconstructed from the RHA1 soil also indicated the presence of  
369 genomic bins (completeness > 70% and contamination < 5%) taxonomically aligned to family  
370 *Sphingomonadaceae*. The genomic bins along with the raw reads obtained for all the five samples  
371 were checked for the presence of *lin* genes (Fig. S8). We observed the presence significant number  
372 of reads corresponding to the *linGH* and *linJ* genes, which encode the acyl-CoA transferase and  
373 thiolase required for the conversion of  $\beta$ -ketoacid to succinyl-CoA and acetyl-CoA. Further,  
374 reads corresponding to *linK*, *linL*, *linM*, and *linN* genes encode a permease, ATPase, periplasmic  
375 protein, and lipoprotein, respectively, and together form a putative ABC-type transporter system  
376 (PMID:17369300). This system is required for the utilization of  $\gamma$ -HCH, probably by conferring  
377 tolerance to toxic dead-end metabolites such as 2,5-DCP (PMID:17369300). Homologues showing  
378 high levels of similarity to the *linKLMN* genes have been found only in *sphingomonads*, suggesting  
379 that their role in active transport of variety of xenobiotic compounds (PMID: 20197499).  
380 Interestingly, the genes involved in upper HCH degradation pathway (transformation of HCH to  
381 2,5-DCP) were either not present or not detected based on reads alignment. Therefore, we can  
382 hypothesize that, under the HCH selection pressure, the communities that can tolerate HCH have  
383 evolved first and these strains are still in a process to acquire the trait of HCH degradation.  
384 However, the functional analysis of the metagenomic sequences revealed the abundance of  
385 monooxygenases (Fig. S9) and RHA1 sample showed the ability of the community to degrade

386 aromatic compounds which could be possible metabolites of HCH (Fig. S10). Therefore, the HCH  
387 may be getting metabolized into further intermediates and the metabolites could subsequently  
388 induced degradation pathways of monooxygenases and enzymes of aromatic degradation  
389 pathways.

## 390 **ENVIRONMENTAL IMPLICATION**

391 Isotope fractionation is almost not affected by concentration changes caused by dilution, sorption  
392 and volatilization, which gives advantage for analyzing mechanisms governing the transformation  
393 of organic contaminants in complex systems. In this study, CSIA and EF could be applied for  
394 characterizing the variability of transformation process of HCHs in a soil-plant system. The  
395 correlation of  $^{13}\text{C}$  and  $^{37}\text{Cl}$  fractionation reveals that the overall transformation processes could be  
396 characterized by one factor  $\Lambda$ , indicating a similar mode of C-Cl bond cleavage, in contrast to  
397 enantiomer fractionation suggesting a changing preference for transformation of  $\alpha$ -HCH  
398 stereoisomers. The combination of multi-element isotope fractionation and EF may provide clues  
399 to identify transformation mechanisms in more detail in future studies.

400 HCHs could serve as an example of persistent environmental contaminants and the developed  
401 concept is also beneficial for identifying the transformation processes of other organic pollutants  
402 in complex systems, such as soil-plant system, or food webs.

403 Phytoremediation is based on the cooperation of plants and their associated microorganisms. It has  
404 been regarded as an efficient option for the clean-up of contaminants in soil <sup>46,47</sup>. Our study shows  
405 the potential of transforming  $\alpha$ -HCH in the soil-wheat system, which gives a strong evidence of  
406 phytoremediation related not only to the uptake but also the transformation of  $\alpha$ -HCH. The  
407 phytoremediation of HCHs by the uptake account for a small part of the total loss <sup>24,48</sup>, but it may

408 be important to be considered for a more complete picture in the future. However, the isotope study  
409 demonstrates that the transformation of organic pollutants needs to be taken into account next to  
410 uptake. CSIA and EF provide a great potential for detecting the previously non-considered  
411 transformation process of  $\alpha$ -HCH in soil-plant systems.

412

413 **AUTHOR INFORMATION**

414 **Corresponding Author**

415 \*Phone: +49-3412351212; fax: +49-341451212; e-mail: [hans.richnow@ufz.de](mailto:hans.richnow@ufz.de).

416 **ORCID**

417 Xiao Liu: 0000-0002-5363-6331

418 Langping Wu: 0000-0003-0599-7172

419 Steffen Kümmel: 0000-0002-8114-8116

420 Hans-Hermann Richnow: 0000-0002-6144-4129

421 **Author Contributions**

422 The manuscript was written through contributions of all authors. All authors have given approval  
423 to the final version of the manuscript.

424 **Notes**

425 The authors declare no competing financial interest.

426 **ACKNOWLEDGEMENTS**

427 Xiao Liu (File No. 201703250070) is financially supported by the China Scholarship Council. This  
428 work was supported by the German-Israeli Foundation for Scientific Research and Development  
429 (GIF) [Grant no. I-1368-307.8/2016]. We are thankful for the use of the analytical facilities of the  
430 Centre for Chemical Microscopy (ProVIS) at UFZ Leipzig, which is supported by European

431 Regional Development Funds (EFRE-Europe funds Saxony) and the Helmholtz Association. We  
432 are thankful to Matthias Gehre for support in the Isotope Laboratory.

### 433 **Supporting Information**

434 Details on experimental conditions, extraction methods, and analytic methods; concentration,  
435 metabolites and metagenome analysis.

436

### 437 **References**

438 (1) Kumar, M.; Gupta, S. K.; Garg, S. K.; Kumar, A. Biodegradation of  
439 Hexachlorocyclohexane-Isomers in Contaminated Soils. *Soil Biol. Biochem.* **2006**, *38* (8),  
440 2318–2327.

441 (2) Vijgen, J.; Abhilash, P. C.; Li, Y. F.; Lal, R.; Forter, M.; Torres, J.; Singh, N.; Yunus, M.;  
442 Tian, C.; Schäffer, A. Weber, R. Hexachlorocyclohexane ( HCH ) as New Stockholm  
443 Convention POPs — a Global Perspective on the Management of Lindane and Its Waste  
444 Isomers. *Environ. Sci. Pollut. Res.* **2011**, *18*, 152–162.

445 (3) Kumar Maurya, A.; Kumar, A.; Joseph, P. E. Trends in Ambient Loads of DDT and HCH  
446 Residues in Animal's and Mother's Milk of Paliakalan Kheeri, Uttar Pradesh-India. *Int. J.*  
447 *Sci. Res. Publ.* **2013**, *3* (1), 2250–3153.

448 (4) Stone, W. F. G. A.; Abel, E. W.; Oxford, P.; Moller, K.; Bretzke, C.; Kopf, J.; Rimkus, G.  
449 The Absolute Configuration of ( + )- $\alpha$ -1,2,3,4,5,6-Hexachlorocyclohexane, and Its  
450 Permeation through the Seal Blood-Brain Barrier. *Angew. Chem. Int. Ed. Engl.* **1994**, *33*,  
451 882–884.

- 452 (5) Romanić, S. H.; Marenjak, T. S.; Klinčić, D.; Janicki, Z.; Srebočan, E.; Konjević, D.  
453 Organochlorine Compounds in Red Deer (*Cervus Elaphus L.*) and Fallow Deer (*Dama*  
454 *Dama L.*) from Inland and Coastal Croatia. *Environ. Monit. Assess.* **2012**, *184* (8), 5173–  
455 5180.
- 456 (6) Tomza-Marciniak, A.; Marciniak, A.; Pilarczyk, B.; Prokulewicz, A.; Bąkowska, M.  
457 Interspecies Comparison of Chlorinated Contaminant Concentrations and Profiles in Wild  
458 Terrestrial Mammals from Northwest Poland. *Arch. Environ. Contam. Toxicol.* **2014**, *66*  
459 (4), 491–503.
- 460 (7) Dettenmaier, E. M.; Bugbee, B. Chemical Hydrophobicity and Uptake by Plant Roots.  
461 *Environ. Sci. Technol.* **2009**, *43* (2), 324–329.
- 462 (8) Trapp, S. Calibration of a Plant Uptake Model with Plant- and Site-Specific Data for  
463 Uptake of Chlorinated Organic Compounds into Radish. *Environ. Sci. Technol.* **2015**, *49*  
464 (1), 395–402.
- 465 (9) Singh, N. Enhanced Degradation of Hexachlorocyclohexane Isomers in Rhizosphere Soil  
466 of *Kochia Sp.* *Bull. Environ. Contam. Toxicol.* **2003**, *70* (4), 775–782.
- 467 (10) Verma, H.; Kumar, R.; Oldach, P.; Sangwan, N.; Khurana, J. P.; Gilbert, J. a; Lal, R.  
468 Comparative Genomic Analysis of Nine *Sphingobium* Strains: Insights into Their  
469 Evolution and Hexachlorocyclohexane (HCH) Degradation Pathways. *BMC Genomics*  
470 **2014**, *15* (1), 1014.
- 471 (11) Zhu, X.; Ni, X.; Waigi, M. G.; Liu, J.; Sun, K.; Gao, Y. Biodegradation of Mixed PAHs  
472 by PAH-Degrading Endophytic Bacteria. *Int. J. Environ. Res. Public Health* **2016**, *13*,



- 473 805.
- 474 (12) Liu, J.; Liu, S.; Sun, K.; Sheng, Y.; Gu, Y.; Gao, Y. Colonization on Root Surface by a  
475 Phenanthrene-Degrading Endophytic Bacterium and Its Application for Reducing Plant  
476 Phenanthrene Contamination. *PLoS One* **2014**, *9* (9), e108249.
- 477 (13) Jian, W.; Juan, L.; Wanting, L.; Qingguo, H.; Yanzheng, G. Science of the Total  
478 Environment Composite of PAH-Degrading Endophytic Bacteria Reduces Contamination  
479 and Health Risks Caused by PAHs in Vegetables. *Sci. Total Environ.* **2017**, *598*, 471–478.
- 480 (14) He, Y.; Langenhoff, A. A. M.; Sutton, N. B.; Rijnaarts, H. H. M.; Blokland, M. H.; Chen,  
481 F.; Huber, C.; Schröder, P. Metabolism of Ibuprofen by *Phragmites Australis*: Uptake and  
482 Phytodegradation. *Environ. Sci. Technol.* **2017**, *51* (8), 4576–4584.
- 483 (15) Nijenhuis, I.; Renpenning, J.; Kümmel, S.; Richnow, H. H.; Gehre, M. Recent Advances  
484 in Multi-Element Compound-Specific Stable Isotope Analysis of Organohalides:  
485 Achievements, Challenges and Prospects for Assessing Environmental Sources and  
486 Transformation. *Trends Environ. Anal. Chem.* **2016**, *11*, 1–8.
- 487 (16) Vogt, C.; Dorer, C.; Musat, F.; Richnow, H. ScienceDirect Multi-Element Isotope  
488 Fractionation Concepts to Characterize the Biodegradation of Hydrocarbons — from  
489 Enzymes to the Environment. *Curr. Opin. Biotechnol.* **2016**, *41*, 90–98.
- 490 (17) Bashir, S.; Hitzfeld, K. L.; Gehre, M.; Richnow, H. H.; Fischer, A. Evaluating  
491 Degradation of Hexachlorocyclohexane (HCH) Isomers within a Contaminated Aquifer  
492 Using Compound-Specific Stable Carbon Isotope Analysis (CSIA). *Water Res.* **2015**, *71*,  
493 187–196.

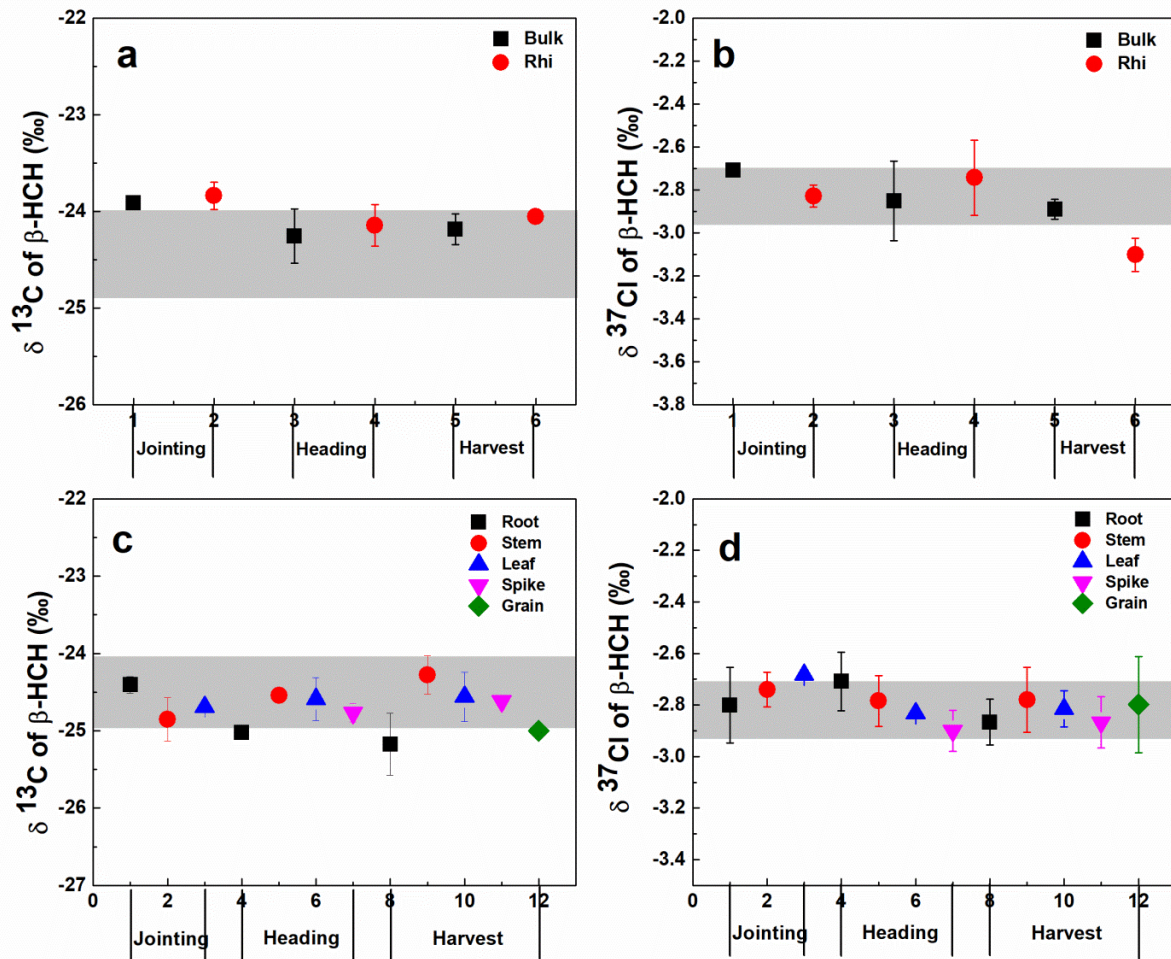
- 494 (18) Lian, S.; Nikolausz, M.; Nijenhuis, I.; Francisco Leite, A.; Richnow, H. H.  
495 Biotransformation and Inhibition Effects of Hexachlorocyclohexanes during Biogas  
496 Production from Contaminated Biomass Characterized by Isotope Fractionation Concepts.  
497 *Bioresour. Technol.* **2018**, *250* (November 2017), 683–690.
- 498 (19) Buser, H. R.; MÜLLER, M. D. Isomer and Enantioselective Degradation of  
499 Hexachlorocyclohexane Isomers in Sewage Sludge under Anaerobic Conditions. *Environ.*  
500 *Sci. Technol.* **1995**, *29* (3), 664–672.
- 501 (20) Liu, Y.; Bashir, S.; Stollberg, R.; Trabitzzsch, R.; Weiß, H.; Paschke, H.; Nijenhuis, I.;  
502 Richnow, H. H. Compound Specific and Enantioselective Stable Isotope Analysis as  
503 Tools to Monitor Transformation of Hexachlorocyclohexane (HCH) in a Complex Aquifer  
504 System. *Environ. Sci. Technol.* **2017**, *51* (16), 8909–8916.
- 505 (21) Wu, L.; Liu, Y.; Liu, X.; Bajaj, A.; Sharma, M.; Lal, R.; Richnow, H. H. Isotope  
506 Fractionation Approach to Characterize the Reactive Transport Processes Governing the  
507 Fate of Hexachlorocyclohexanes at a Contaminated Site in India. *Environ. Int.* **2019**, *132*  
508 (July), 105036.
- 509 (22) Liu, X.; Wu, L.; Kümmel, S.; Richnow, HH. Characterizing the Biotransformation of  
510 Hexachlorocyclohexane in Wheat Using Compound-Specific Stable Isotope Analysis and  
511 Enantiomer Fraction. *J. Hazard. Mater.* **2020**, Under review.
- 512 (23) Zhu, H.; Sun, H.; Yao, Y.; Wang, F.; Zhang, Y.; Liu, X. Fate and Adverse Effects of  
513 Hexabromocyclododecane Diastereoisomers (HBCDDs) in a Soil-Ryegrass Pot System.  
514 *Chemosphere* **2017**, *184*, 452–459.

- 515 (24) Kidd, P. S.; Prieto-Fernández, A.; Monterroso, C.; Acea, M. J. Rhizosphere Microbial  
516 Community and Hexachlorocyclohexane Degradative Potential in Contrasting Plant  
517 Species. *Plant Soil* **2008**, *302* (1–2), 233–247.
- 518 (25) Wu, L.; Moses, S.; Liu, Y.; Renpenning, J.; Richnow, H. H. A Concept for Studying the  
519 Transformation Reaction of Hexachlorocyclohexanes in Food Webs Using Multi-Element  
520 Compound-Specific Isotope Analysis. *Anal. Chim. Acta* **2019**, *1064*, 56–64.
- 521 (26) Horst, A. Compound Specific Stable Chlorine Isotopic Analysis of Volatile Aliphatic  
522 Compounds Using Gas Chromatography Hyphenated with Multiple Collector Inductively  
523 Coupled Plasma Mass Spectrometry. *Anal. Chem.* **2017**, *89*, 9131–9138.
- 524 (27) Badea, S. L.; Vogt, C.; Gehre, M.; Fischer, A.; Danet, A. F.; Richnow, H. H. Development  
525 of an Enantiomer-Specific Stable Carbon Isotope Analysis (ESIA) Method for Assessing  
526 the Fate of  $\alpha$ -Hexachlorocyclo-Hexane in the Environment. *Rapid Commun. Mass*  
527 *Spectrom.* **2011**, *25* (10), 1363–1372.
- 528 (28) Elsner, M.; Jochmann, M. A. Current Challenges in Compound-Specific Stable Isotope  
529 Analysis of Environmental Organic Contaminants. *Anal. Bioanal. Chem.* **2012**, 2471–  
530 2491.
- 531 (29) Wenzel, W. W. Rhizosphere Processes and Management in Plant-Assisted Bioremediation  
532 (Phytoremediation) of Soils. *Plant Soil* **2009**, *321* (1–2), 385–408.
- 533 (30) Namiki, S.; Otani, T.; Seike, N.; Satoh, S. Differential Uptake and Translocation of  $\beta$ -  
534 HCH and Dieldrin by Several Plant Species from Hydroponic Medium. *Environ. Toxicol.*  
535 *Chem.* **2015**, *34* (3), 536–544.

- 536 (31) Su, Y.; Liang, Y. Foliar Uptake and Translocation of Formaldehyde with Bracket Plants  
537 (Chlorophytum Comosum). *J. Hazard. Mater.* **2015**, *291*, 120–128.
- 538 (32) Feng, N. X.; Yu, J.; Zhao, H. M.; Cheng, Y. T.; Mo, C. H.; Cai, Q. Y.; Li, Y. W.; Li, H.;  
539 Wong, M. H. Efficient Phytoremediation of Organic Contaminants in Soils Using Plant–  
540 Endophyte Partnerships. *Sci. Total Environ.* **2017**, *583*, 352–368.
- 541 (33) Gerhardt, K. E.; Huang, X. D.; Glick, B. R.; Greenberg, B. M. Phytoremediation and  
542 Rhizoremediation of Organic Soil Contaminants: Potential and Challenges. *Plant Sci.*  
543 **2009**, *176* (1), 20–30.
- 544 (34) Susarla, S.; Medina, V. F.; Mccutcheon, S. C. Phytoremediation : An Ecological Solution  
545 to Organic Chemical Contamination. *Ecol. Eng.* **2002**, *18*, 647–658.
- 546 (35) Dec, J. Use of Plant Material for the Decontamination of Water Polluted with Phenols.  
547 *Biotechnol. Bioeng.* **1994**, *44*, 1132–1139.
- 548 (36) San Miguel, A.; Schröder, P.; Harpaintner, R.; Gaude, T.; Ravanel, P.; Raveton, M.  
549 Response of Phase II Detoxification Enzymes in Phragmites Australis Plants Exposed to  
550 Organochlorines. *Environ. Sci. Pollut. Res.* **2013**, *20* (5), 3464–3471.
- 551 (37) Becerra-Castro, C.; Kidd, P. S.; Prieto-Fernández, Á.; Weyens, N.; Acea, M. J.;  
552 Vangronsveld, J. Endophytic and Rhizoplane Bacteria Associated with Cytisus Striatus  
553 Growing on Hexachlorocyclohexane-Contaminated Soil: Isolation and Characterisation.  
554 *Plant Soil* **2011**, *340* (1), 413–433.
- 555 (38) Kopinke, F.; Georgi, A.; Imfeld, G.; Richnow, H. Chemosphere Isotope Fractionation of  
556 Benzene during Partitioning e Revisited. *Chemosphere* **2017**, *168*, 508–513.

- 557 (39) Hardoim, P. R.; van Overbeek, L. S.; Elsas, J. D. van. Properties of Bacterial Endophytes  
558 and Their Proposed Role in Plant Growth. *Trends Microbiol.* **2008**, *16* (10), 463–471.
- 559 (40) Law, S. A.; Bidleman, T. F.; Martin, M. J.; Ruby, M. V. Evidence of Enantioselective  
560 Degradation of  $\alpha$ -Hexachlorocyclohexane in Groundwater. *Environ. Sci. Technol.* **2004**,  
561 *38* (6), 1633–1638.
- 562 (41) Bashir, S.; Fischer, A.; Nijenhuis, I.; Richnow, H. H. Enantioselective Carbon Stable  
563 Isotope Fractionation of Hexachlorocyclohexane during Aerobic Biodegradation by  
564 *Sphingobium* Spp. *Environ. Sci. Technol.* **2013**, *47* (20), 11432–11439.
- 565 (42) Suar, M.; Hauser, A.; Poiger, T.; Buser, H. R.; Müller, M. D.; Dogra, C.; Raina, V.;  
566 Holliger, C.; Van Der Meer, J. R.; Lal, R. Kohler, H.P.E. Enantioselective Transformation  
567 of  $\alpha$ -Hexachlorocyclohexane by the Dehydrochlorinases LinA1 and LinA2 from the Soil  
568 Bacterium *Sphingomonas Paucimobilis* B90A. *Appl. Environ. Microbiol.* **2005**, *71* (12),  
569 8514–8518.
- 570 (43) Liu, Y.; Wu, L.; Kohli, P.; Kumar, R.; Stryhanyuk, H.; Nijenhuis, I.; Lal, R.; Richnow,  
571 H.-H. Enantiomer and Carbon Isotope Fractionation of  $\alpha$ -Hexachlorocyclohexane by  
572 *Sphingobium Indicum* Strain B90A and the Corresponding Enzymes. *Environ. Sci.*  
573 *Technol.* **2019**, *53*, 8715–8724.
- 574 (44) Dunfield, K. E.; Germida, J. J. Seasonal Changes in the Rhizosphere Microbial  
575 Communities Associated with Field-Grown Genetically Modified Canola (*Brassica*  
576 *Napus*). *Appl. Environ. Microbiol.* **2003**, *69* (12), 7310–7318.
- 577 (45) Lal, R.; Pandey, G.; Sharma, P.; Kumari, K.; Malhotra, S.; Pandey, R.; Raina, V.; Kohler,

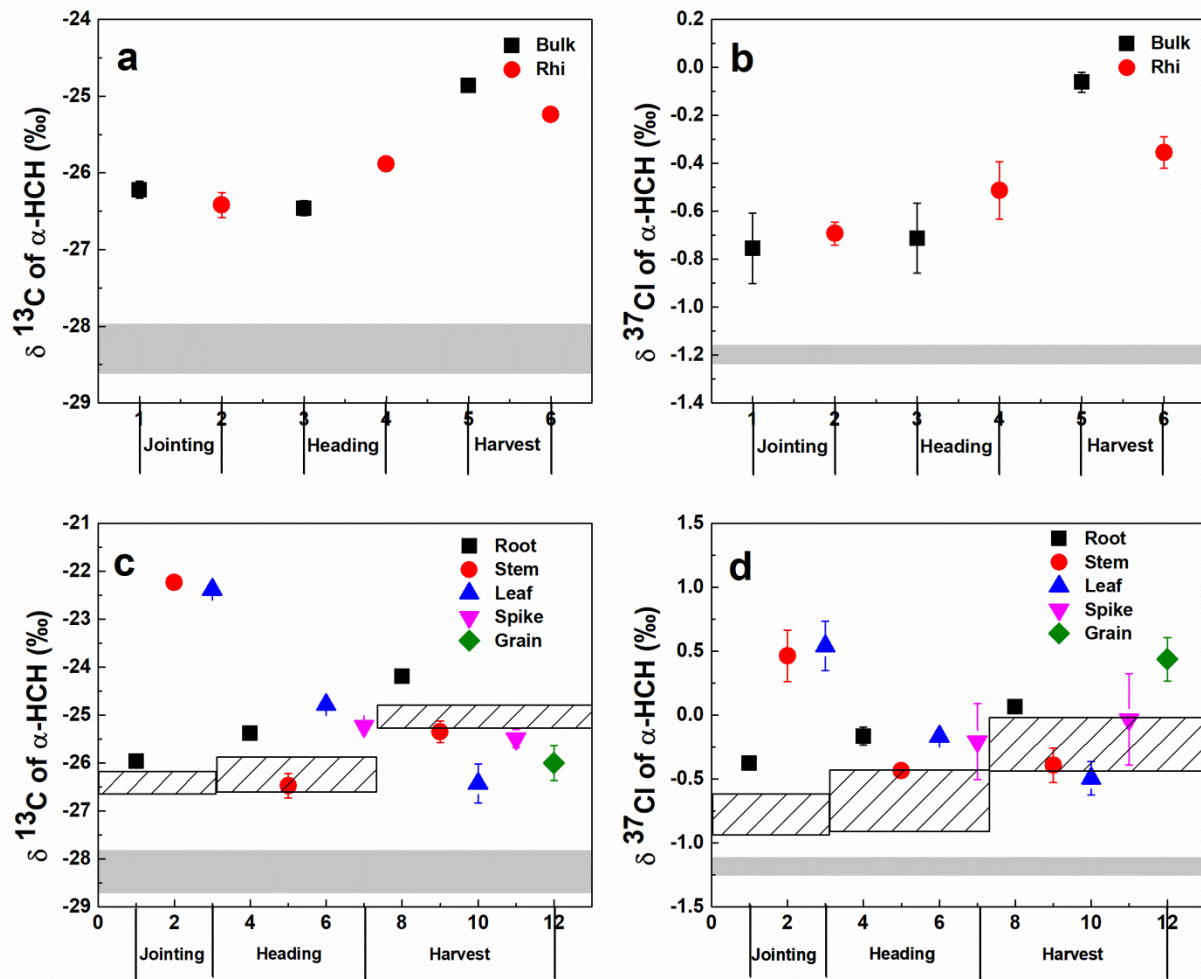
- 578 H.-P. E.; Holliger, C.; Jackson, C.; et al. Biochemistry of Microbial Degradation of  
579 Hexachlorocyclohexane and Prospects for Bioremediation. *Microbiol. Mol. Biol. Rev.*  
580 **2010**, *74* (1), 58–80.
- 581 (46) Fester, T.; Giebler, J.; Wick, L. Y.; Schlosser, D.; Kästner, M. Plant-Microbe Interactions  
582 as Drivers of Ecosystem Functions Relevant for the Biodegradation of Organic  
583 Contaminants. *Curr. Opin. Biotechnol.* **2014**, *27*, 168–175.
- 584 (47) Arslan, M.; Imran, A.; Khan, Q. M.; Afzal, M. Plant–Bacteria Partnerships for the  
585 Remediation of Persistent Organic Pollutants. *Environ. Sci. Pollut. Res.* **2017**, *24* (5),  
586 4322–4336.
- 587 (48) Becerra-Castro, C.; Prieto-Fernández, Á.; Kidd, P. S.; Weyens, N.; Rodríguez-Garrido, B.;  
588 Touceda-González, M.; Acea, M. J.; Vangronsveld, J. Improving Performance of *Cytisus*  
589 *Striatus* on Substrates Contaminated with Hexachlorocyclohexane (HCH) Isomers Using  
590 Bacterial Inoculants: Developing a Phytoremediation Strategy. *Plant Soil* **2013**, *362* (1–2),  
591 247–260.



592

593 Fig. 1. Carbon (a) and chlorine (b) isotope composition of  $\beta$ -HCH in the bulk soil and the  
 594 rhizosphere soil. Carbon (c) and chlorine (d) isotope composition of  $\beta$ -HCH in wheat tissues. The  
 595 grey bar shows the range of the isotope values of  $\beta$ -HCH spiked to the original soil samples. Error  
 596 bars represent SD values.

597

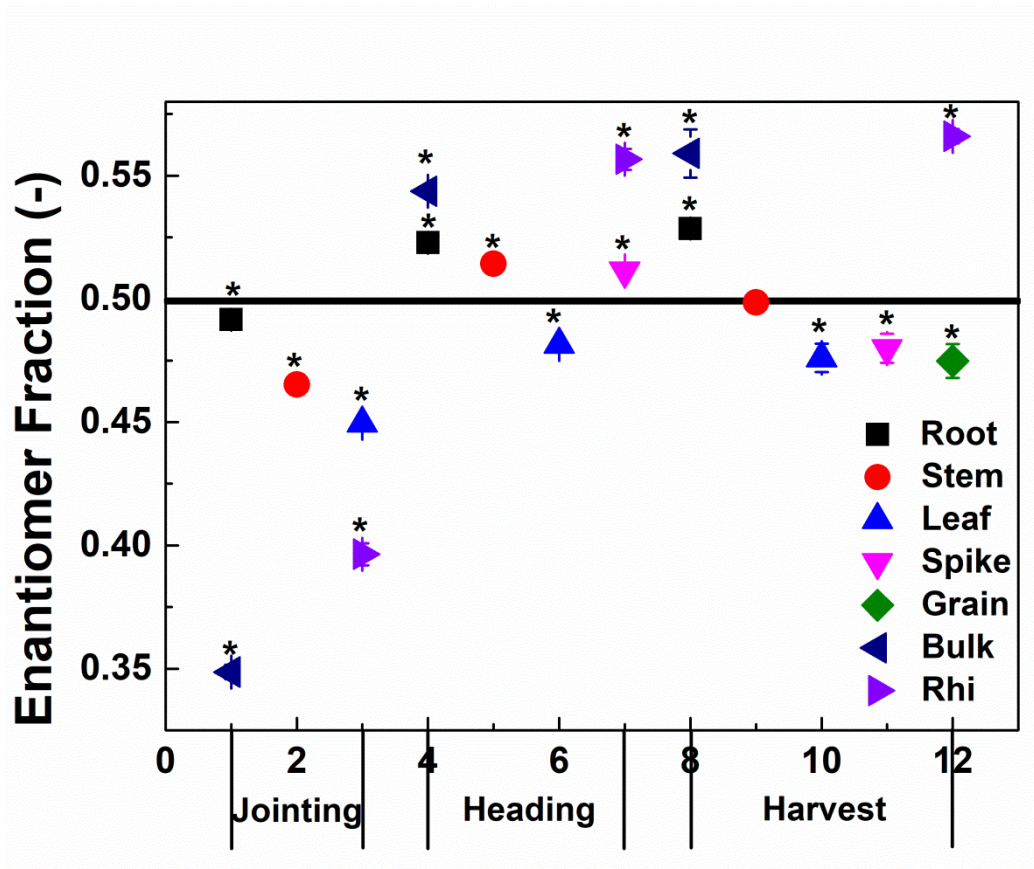


598

599 Fig. 2. Carbon (a) and chlorine (b) isotope composition of  $\alpha\text{-HCH}$  in the bulk soil and the  
 600 rhizosphere soil. Carbon (c) and chlorine (d) isotope composition of  $\alpha\text{-HCH}$  in wheat tissues. The  
 601 grey bar shows the isotopic range of  $\alpha\text{-HCH}$  spiked to the original soil samples. The stripe bar  
 602 shows the range of isotope values of  $\alpha\text{-HCH}$  in bulk and rhizosphere soil at different wheat growth  
 603 stages. Error bars represent SD values.

604

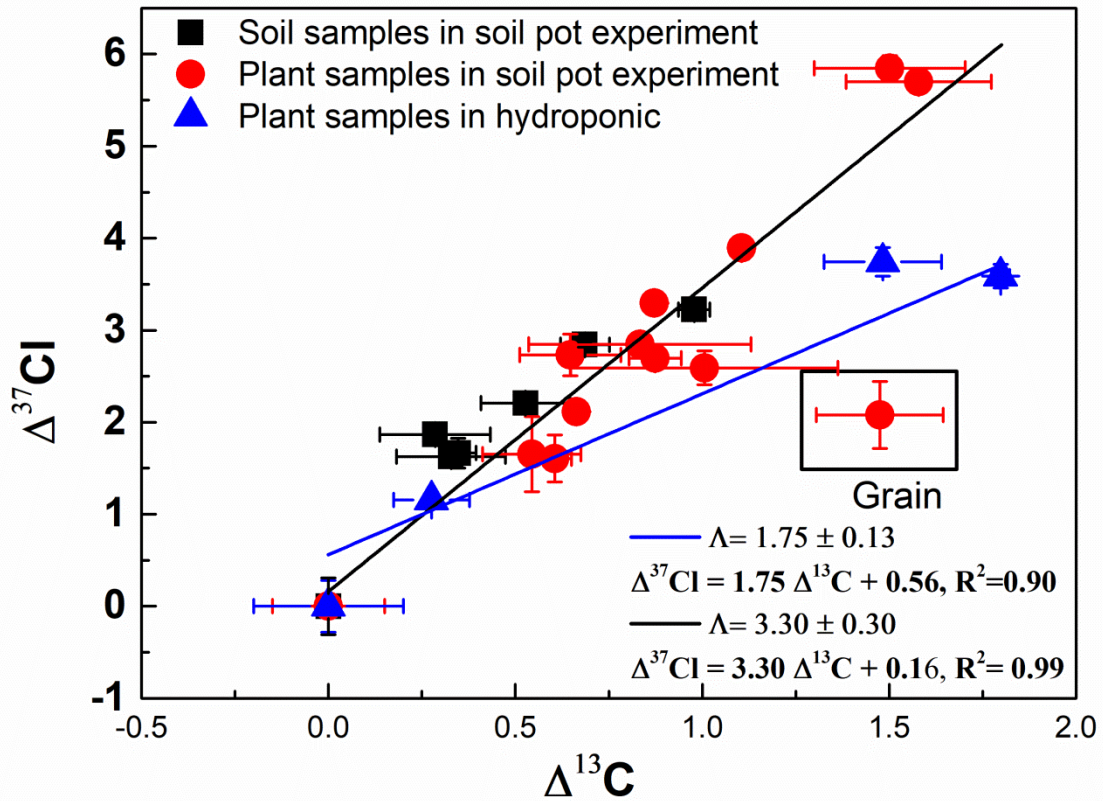




605

606 Fig. 3. Enantiomer fractionation of  $\alpha$ -HCH in different wheat tissues and soil. The bar is showing  
 607 the EF values of the racemic mixture spiked to the soil. Bulk means bulk soil. Rhi means  
 608 rhizosphere soil. The asterisk refers to the significant difference between EF(-) in soil and plant  
 609 samples compared with that in HCH used for spiking according to independent *t*-test ( $p < 0.05$ ).  
 610 Error bars represent SD values.

611



612

613 Fig. 4. Dual element analysis (C-Cl) of  $\alpha$ -HCH in soil and wheat tissues. The isotope data of  $\alpha$ -  
 614 HCH in plant samples in hydroponic experiment was obtained from elsewhere<sup>24</sup>. The  $\Delta$  indicates  
 615 the differences in isotope values ( $\delta$ ) between the initial isotope composition of HCH used for  
 616 spiking ( $\delta_0$ ) and the isotope composition of HCH at each sampling point ( $\delta_t$ ),  $\Delta = \delta_t - \delta_0$ . The  
 617 same HCH standard was used for spiking in the soil pot and hydroponic experiments. Error bars  
 618 represent SD values.

619